

Analysis of mesoscopic loss effects in anisotropic poroelastic media using harmonic finite element simulations

Juan E. Santos,[†] Stefano Picotti^{*} and José M. Carcione^{*}

[†] CONICET, Instituto del Gas y del Petróleo, Universidad de Buenos Aires, Argentina
and Department of Mathematics, Purdue University.

^{*} Istituto Nazionale di Oceanografia e di Geofisica Sperimentale - OGS, Trieste, Italy

SEG Annual Meeting, San Antonio, Texas, September 21st 2011

Anisotropic poroelasticity and mesoscopic loss. I

- Reservoirs rocks consists usually of **thinly layered** fluid-saturated poroelastic sediments.
- The traveling P-waves induce fluid-pressure gradients at mesoscopic-scale heterogeneities, generating interlayer **fluid flow and slow (diffusion)** Biot waves (**mesoscopic loss mechanism**).
- These finely layered sediments behave like **viscoelastic transversely isotropic (VTI)** media at long wavelengths.

Anisotropic poroelasticity and mesoscopic loss. II

- For fluid-saturated poroelastic media (Biot's media), White et al. (1975) were the first to introduce the mesoscopic-loss mechanism in the framework of Biot's theory.
- Gelinsky and Shapiro (GPY, 62, 1997) obtained the relaxed and unrelaxed stiffnesses of the equivalent poro-viscoelastic medium to a **finely layered horizontally homogeneous (FLHH)** Biot's medium.
- For a **FLHH** Biot's medium, Krzikalla and Müller (GPY, 76, 2011) combined the two previous models to obtain the **five** complex and frequency-dependent stiffnesses of the **equivalent VTI medium**.

Anisotropic poroelasticity and mesoscopic loss. III

- Krzikalla and Müller assumed fluid-flow direction perpendicular to the layering plane. Hence, the model uses only one relaxation function, associated with the symmetry-axis P-wave stiffness.
- To test the model and provide a more general modeling tool, we present a **numerical upscaling procedure** to obtain the complex stiffnesses of the effective VTI medium.
- The method uses the Finite Element Method (**FEM**) to solve **Biot's equation of motion** in the space-frequency domain with boundary conditions representing **compressibility and shear harmonic** experiments.

Anisotropic poroelasticity and mesoscopic loss. IV

- The methodology is applied to the Utsira aquifer of the North Sea, where CO_2 has been injected during the last 15 years.
- The example considers a sequence of gas-saturated sandstone and mudstone layers, representing models of the reservoir and cap rock of the aquifer system.
- The quality factors and velocities as a function of frequency and propagation angle are tested against those provided by the theory for laterally homogeneous layers.
- Examples for highly heterogeneous Biot's media are also presented.

TIV media and fine layering. I

Let us consider isotropic fluid-saturated poroelastic layers.

$\mathbf{u}^s(\mathbf{x}), \mathbf{u}^f(\mathbf{x})$: time Fourier transform of the displacement vector of the solid and fluid relative to the solid frame, respectively.

$$\mathbf{u} = (\mathbf{u}^s, \mathbf{u}^f)$$

$\sigma_{kl}(u), \mathbf{p}_f(u)$: Fourier transform of the total stress and the fluid pressure, respectively

On each plane layer n in a sequence of N layers, the frequency-domain stress-strain relations are

$$\sigma_{kl}(u) = 2\mu \varepsilon_{kl}(u^s) + \delta_{kl} \left(\lambda_G \nabla \cdot u^s + \alpha M \nabla \cdot u^f \right),$$

$$\mathbf{p}_f(u) = -\alpha M \nabla \cdot u^s - M \nabla \cdot u^f.$$

TIV media and fine layering. II

Biot's equations of motion:

$$\begin{aligned} -\omega^2 \rho u^s(x, \omega) - \omega^2 \rho_f u^f(x, \omega) - \nabla \cdot \sigma(u) &= 0, \\ -\omega^2 \rho u^f(x, \omega) - \omega^2 m u^f(x, \omega) + i\omega \frac{\eta}{\kappa} u^f(x, \omega) + \nabla p_f(u) &= 0, \end{aligned}$$

$\omega = 2\pi f$: angular frequency

$m = \frac{\mathcal{T} \rho_f}{\phi}$: mass coupling coefficient \mathcal{T} : tortuosity factor

$$\rho = (1 - \phi) \rho_s + \phi \rho_f,$$

ρ_s and ρ_f : mass densities of the solid grains and fluid,
respectively

η : fluid viscosity

κ : frame permeability

TIV media and fine layering. III

τ_{ij} : stress tensor of the equivalent VTI medium

Assuming a **closed system**($\nabla \cdot u^f = 0$), the corresponding **stress-strain relations**, stated in the space-frequency domain, are

$$\tau_{11}(u) = p_{11} \epsilon_{11}(u^s) + p_{12} \epsilon_{22}(u^s) + p_{13} \epsilon_{33}(u^s),$$

$$\tau_{22}(u) = p_{12} \epsilon_{11}(u^s) + p_{11} \epsilon_{22}(u^s) + p_{13} \epsilon_{33}(u^s),$$

$$\tau_{33}(u) = p_{13} \epsilon_{11}(u^s) + p_{13} \epsilon_{22}(u^s) + p_{33} \epsilon_{33}(u^s),$$

$$\tau_{23}(u) = 2 p_{55} \epsilon_{23}(u^s),$$

$$\tau_{13}(u) = 2 p_{55} \epsilon_{13}(u^s),$$

$$\tau_{12}(u) = 2 p_{66} \epsilon_{12}(u^s).$$

This approach provides the complex velocities of the fast modes and takes into account **interlayer flow effects**.

TIV media and fine layering. IV

Krzikalla and Müller (GPY, 76, 2011) proposed a model to determine the stiffnesses p_{IJ} for a stack of two thin alternating porous layers.

These analytical p_{IJ} 's will be used to check the results of the **FEM** to be used next to determine these coefficients.

Using the p_{IJ} 's and the thickness weighted average of the bulk density will in turn allow us to determine the **phase velocity and quality factors** for the qP, qS and SH waves.

The harmonic experiments to determine the stiffness coefficients. I

To determine the complex stiffness we solve Biot's equation in the 2D case on a reference square $\Omega = (0, L)^2$ with boundary Γ in the (x_1, x_3) -plane. Set $\Gamma = \Gamma^L \cup \Gamma^B \cup \Gamma^R \cup \Gamma^T$, where

$$\begin{aligned}\Gamma^L &= \{(x_1, x_3) \in \Gamma : x_1 = 0\}, & \Gamma^R &= \{(x_1, x_3) \in \Gamma : x_1 = L\}, \\ \Gamma^B &= \{(x_1, x_3) \in \Gamma : x_3 = 0\}, & \Gamma^T &= \{(x_1, x_3) \in \Gamma : x_3 = L\}.\end{aligned}$$

Over the seismic band of frequencies, the acceleration (ω^2) terms are negligible relative to the viscous resistance and can be discarded, so that we solve the **diffusion Biot's equation**.

ν : the unit outer normal on Γ

χ : a unit tangent on Γ so that $\{\nu, \chi\}$ is an orthonormal system on Γ .

The harmonic experiments to determine the stiffness coefficients. II

The poroelastic fluid-saturated sample is subjected to **time-harmonic compressibility and shear tests** described by the following sets of **boundary conditions**.

$p_{33}(\omega)$:

$$\begin{aligned}\sigma(u)\nu \cdot \nu &= -\Delta P, & (x_1, x_3) &\in \Gamma^T, \\ \sigma(u)\nu \cdot \chi &= 0, & (x_1, x_3) &\in \Gamma^T \cup \Gamma^L \cup \Gamma^R, \\ u^s \cdot \nu &= 0, & (x_1, x_3) &\in \Gamma^L \cup \Gamma^R, \\ u^s &= 0, & (x_1, x_3) &\in \Gamma^B, \quad u^f \cdot \nu = 0, & (x_1, x_3) &\in \Gamma.\end{aligned}$$

Denote by V the original volume of the sample and by $\Delta V(\omega)$ its (complex) oscillatory volume change.

The harmonic experiments to determine the stiffness coefficients. III

In the quasistatic case

$$\frac{\Delta V(\omega)}{V} = -\frac{\Delta P}{p_{33}(\omega)},$$

Then after computing the average $u_3^{s,T}(\omega)$ of the vertical displacements on Γ^T , we approximate

$$\Delta V(\omega) \approx Lu_3^{s,T}(\omega)$$

which enable us to compute $p_{33}(\omega)$

To determine $p_{11}(\omega)$ we solve an identical boundary value problem than for p_{33} but for a 90° rotated sample.

The harmonic experiments to determine the stiffness coefficients. IV

$p_{55}(\omega)$: the boundary conditions are

$$-\sigma(u)\nu = g, \quad (x_1, x_3) \in \Gamma^T \cup \Gamma^L \cup \Gamma^R,$$

$$u^s = 0, \quad (x_1, x_3) \in \Gamma^B,$$

$$u^f \cdot \nu = 0, \quad (x_1, x_3) \in \Gamma,$$

where

$$g = \begin{cases} (0, \Delta G), & (x_1, x_3) \in \Gamma^L, \\ (0, -\Delta G), & (x_1, x_3) \in \Gamma^R, \\ (-\Delta G, 0), & (x_1, x_3) \in \Gamma^T. \end{cases}$$

The harmonic experiments to determine the stiffness coefficients. V

The change in shape suffered by the sample is

$$\tan[\theta(\omega)] = \frac{\Delta G}{p_{55}(\omega)}. \quad (1)$$

$\theta(\omega)$: the angle between the original positions of the lateral boundaries and the location after applying the shear stresses.

Since

$\tan[\theta(\omega)] \approx u_1^{s,T}(\omega)/L$, where $u_1^{s,T}(\omega)$ is the average horizontal displacement at Γ^T , $p_{55}(\omega)$ can be determined from (1)

to determine $p_{66}(\omega)$ (shear waves traveling in the (x_1, x_2) -plane), we rotate the layered sample 90° and apply the shear test as indicated for $p_{55}(\omega)$.

The harmonic experiments to determine the stiffness coefficients. VI

$p_{13}(\omega)$: the boundary conditions are

$$\sigma(u)\nu \cdot \nu = -\Delta P, \quad (x_1, x_3) \in \Gamma^R \cup \Gamma^T,$$

$$\sigma(u)\nu \cdot \chi = 0, \quad (x_1, x_3) \in \Gamma,$$

$$u^s \cdot \nu = 0, \quad (x_1, x_3) \in \Gamma^L \cup \Gamma^B, \quad u^f \cdot \nu = 0, \quad (x_1, x_3) \in \Gamma.$$

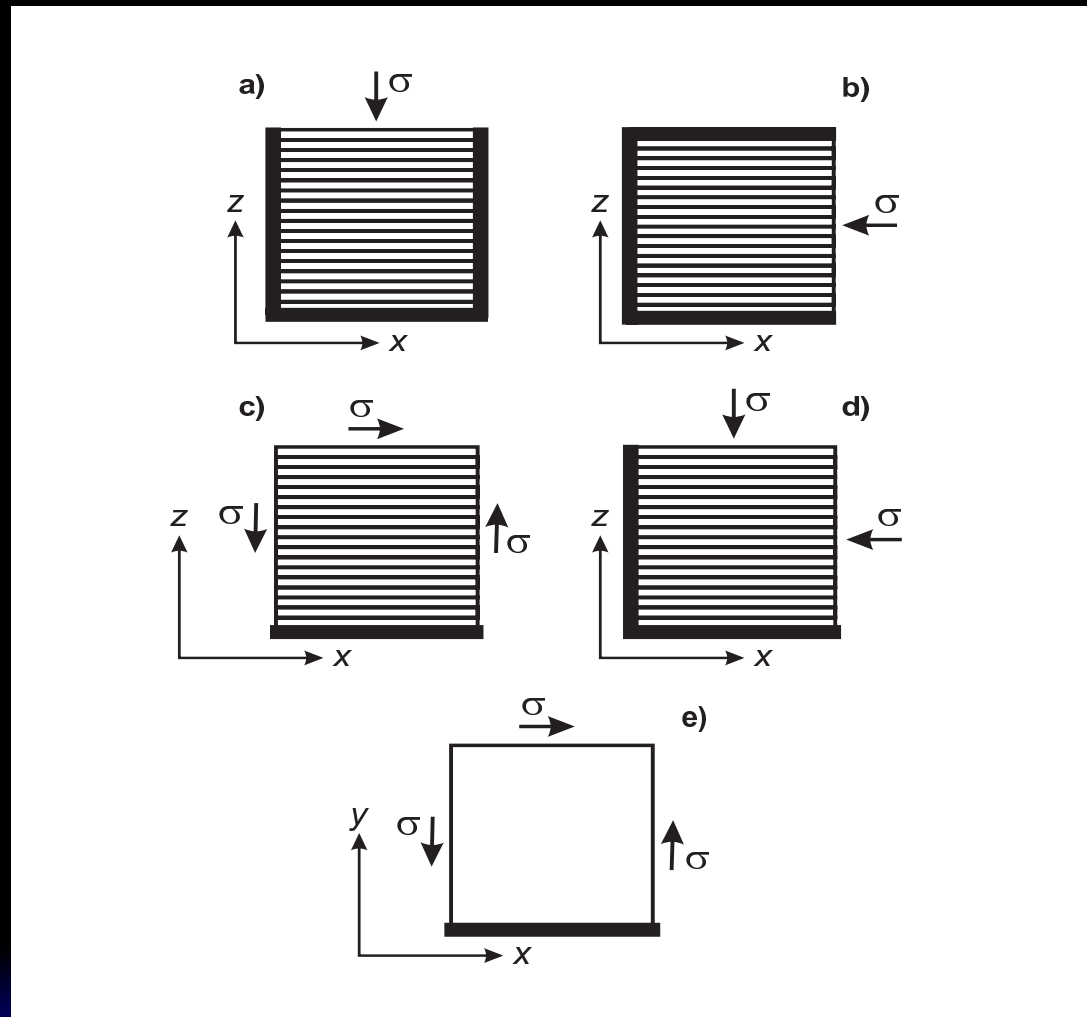
In this experiment $\epsilon_{22} = \nabla \cdot u^f = 0$, so that

$$\tau_{11} = p_{11}\epsilon_{11} + p_{13}\epsilon_{33}, \quad \tau_{33} = p_{13}\epsilon_{11} + p_{33}\epsilon_{33},$$

$\epsilon_{11}, \epsilon_{33}$: the strain components at the right lateral side and top side of the sample, respectively. Then,

$$p_{13}(\omega) = (p_{11}\epsilon_{11} - p_{33}\epsilon_{33}) / (\epsilon_{11} - \epsilon_{33}).$$

Schematic representation of the oscillatory compressibility and shear tests in Ω



Examples. I

Let us consider the **North-Sea Utsira formation** located 800 m below the sea bottom, which contains a highly permeable **sandstone**, where carbon dioxide (**CO₂**) has been injected in the Sleipner field.

Within the Utsira aquifer, compacted **mudstone layers** have been identified, acting as barriers to the upward migration of the **CO₂**.

Examples. II

Properties of the Utsira formation.

	Sandstone	Mudstone
Grain bulk modulus, K_s (GPa)	40	20
density, ρ_s (kg/m ³)	2600	2600
Frame bulk modulus, K_m (GPa)	1.37	7
shear modulus, μ_m (GPa)	0.82	6
porosity, ϕ	0.36	0.2
permeability, κ (D)	1.6	0.01
Brine density, ρ_w (kg/m ³)	1030	1030
viscosity, η_w (Pa s)	0.0012	0.0012
bulk modulus, K_w (GPa)	2.6	2.6
CO ₂ density, ρ_g (kg/m ³)	505	–
viscosity, η_g (Pa s)	0.00015	–
bulk modulus, K_g (MPa)	25	–

Examples. III

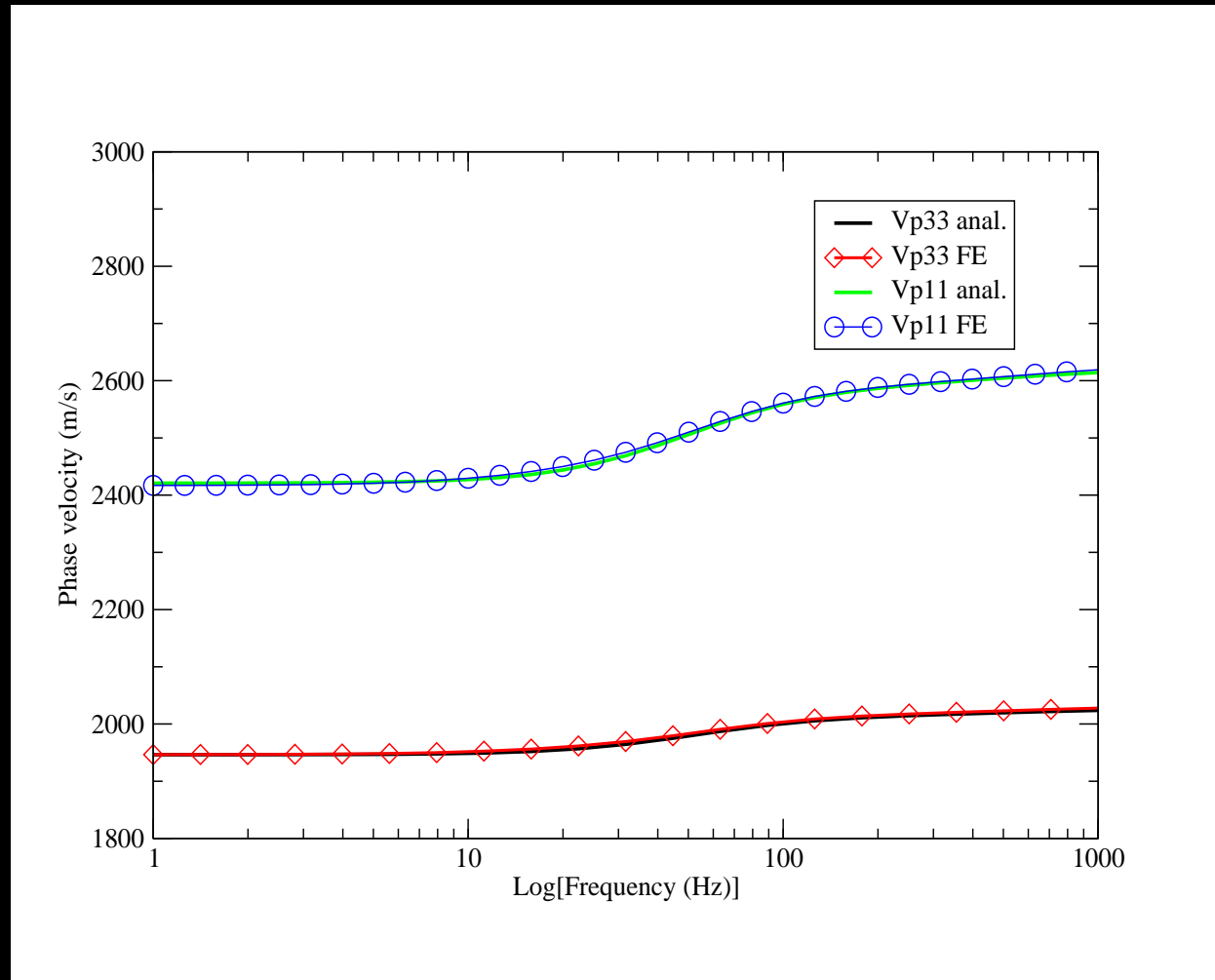
The upper part of the aquifer (cap rock) is the location where the proportion of mudstone may be substantial.

The example considers alternating layers of **brine-saturated mudstone** and **CO₂-saturated sandstone** of thicknesses 5 cm and 1 cm, respectively, and a period of 6 cm.

It models the case in which the original brine has been replaced by **CO₂** and the sequence may represent **possible leakages to the cap rock**.

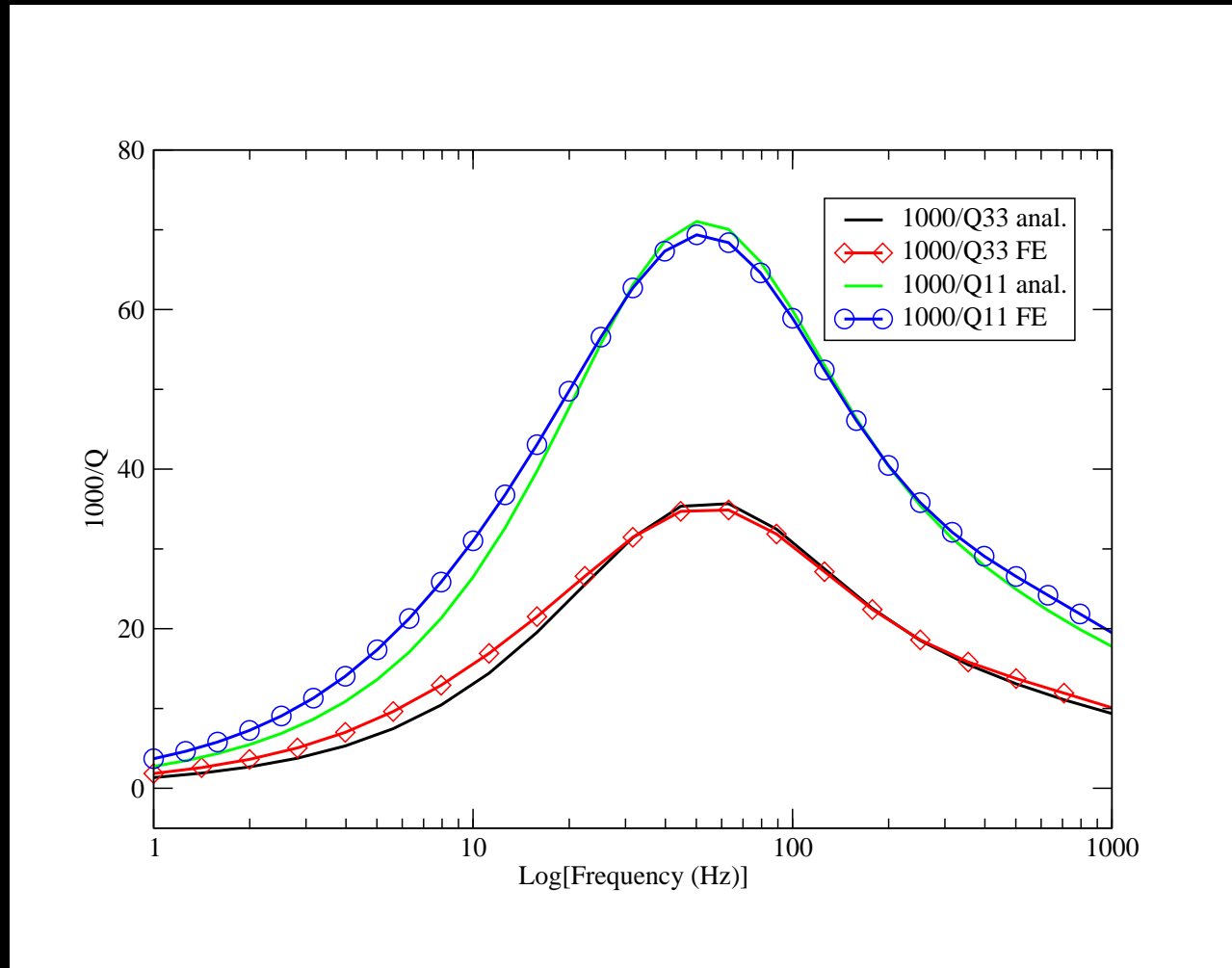
The figures compares the analytical p_{IJ} with the FE solution for several periods of the stratification.

P-wave phase velocities perpendicular (V_{p33}) and parallel (V_{p11}) to the layering plane



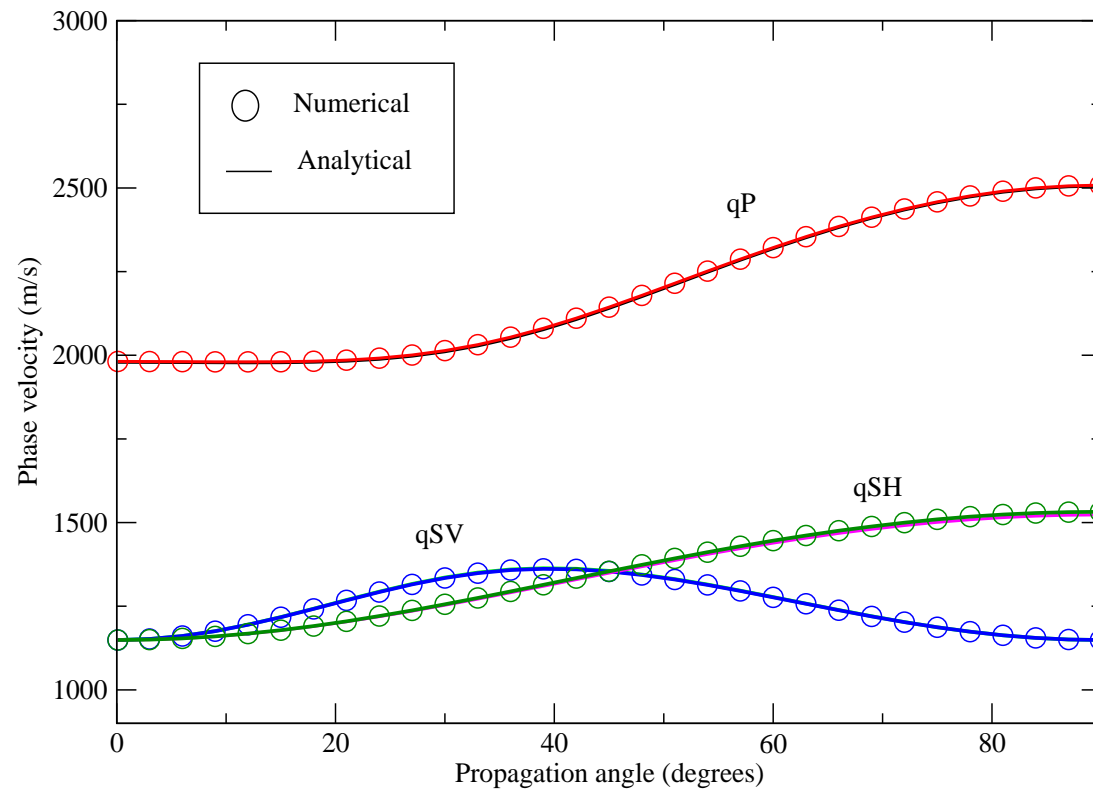
The medium is a sequence of brine-saturated mudstone and CO_2 -saturated sandstone layers with thicknesses of 5 cm and 1 cm, respectively. Symbols indicate FE values.

Dissipation factors perpendicular (1000/Q33) and parallel (1000/Q11) to the layering plane



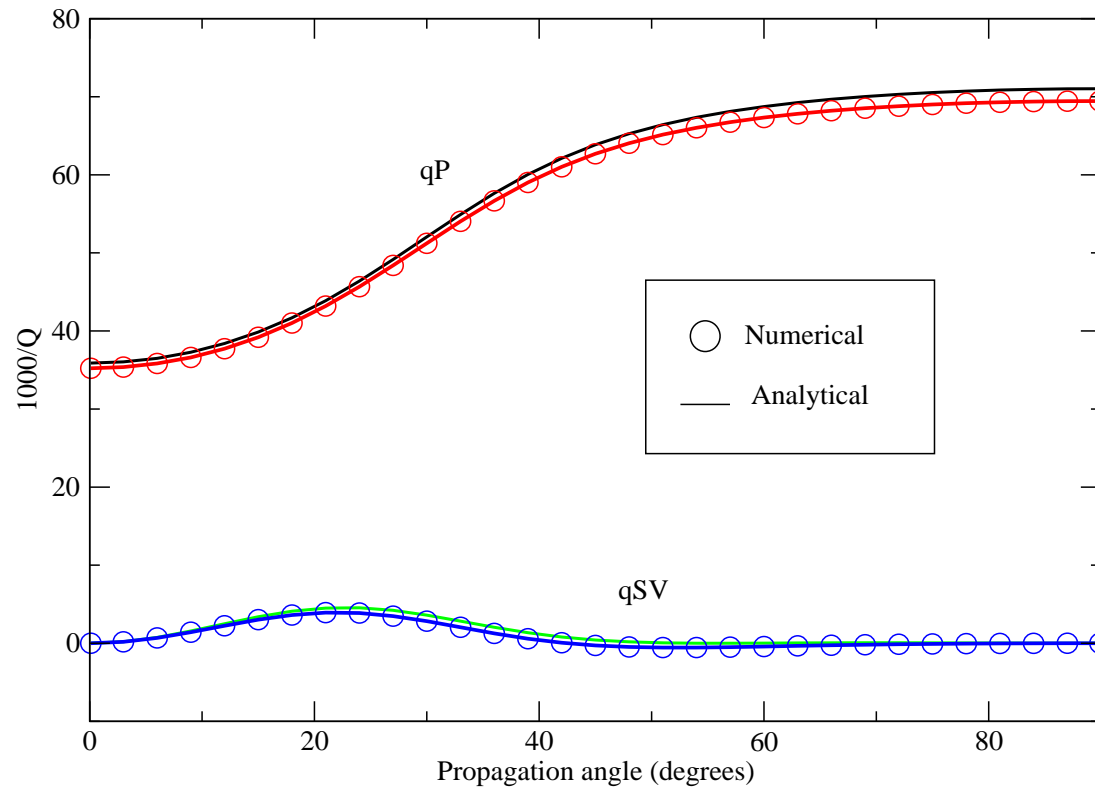
The medium is a sequence of brine-saturated mudstone and CO₂-saturated sandstone layers with thicknesses of 5 cm and 1 cm, respectively. Symbols indicate FE values.

Phase velocities at 50 Hz as function of the propagation angle



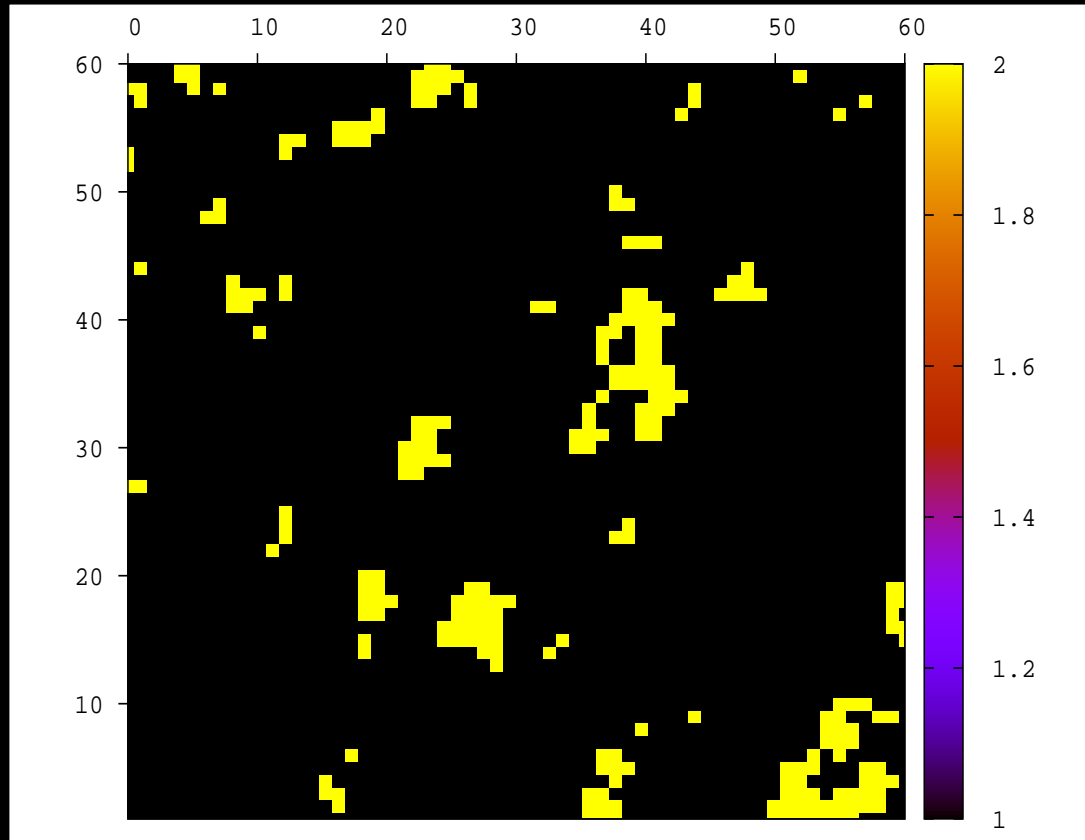
The medium is a sequence of mudstone and CO₂-saturated sandstone layers with thicknesses of 5 cm and 1 cm, respectively

Dissipation factors at 50 Hz as function of the propagation angle



The medium is a sequence of mudstone and CO₂-saturated sandstone layers with thicknesses of 5 cm and 1 cm, respectively

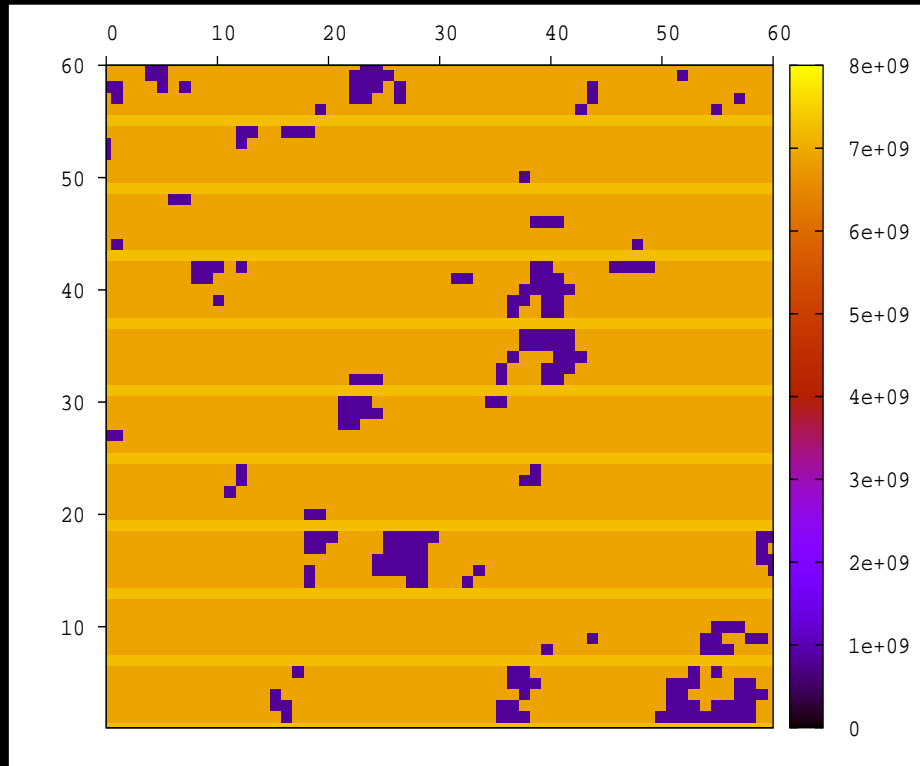
PATCHY SATURATION. CO₂-BRINE DISTRIBUTION



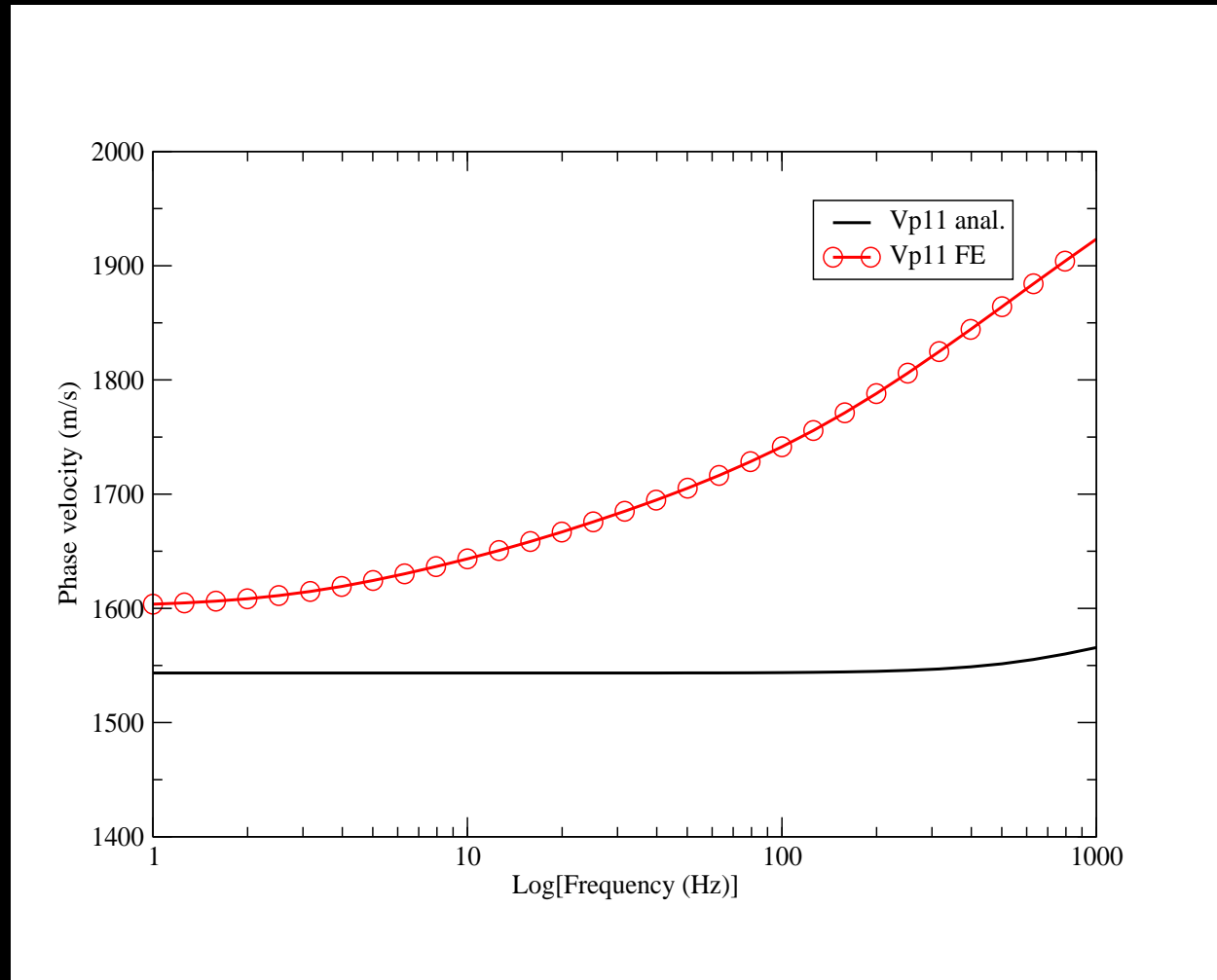
Yellow zones correspond to CO₂ saturation and the black ones to pure brine saturation.

The overall CO₂ saturation is 7 percent.

PATCHY SATURATION. Coefficient λ_G (Pa)

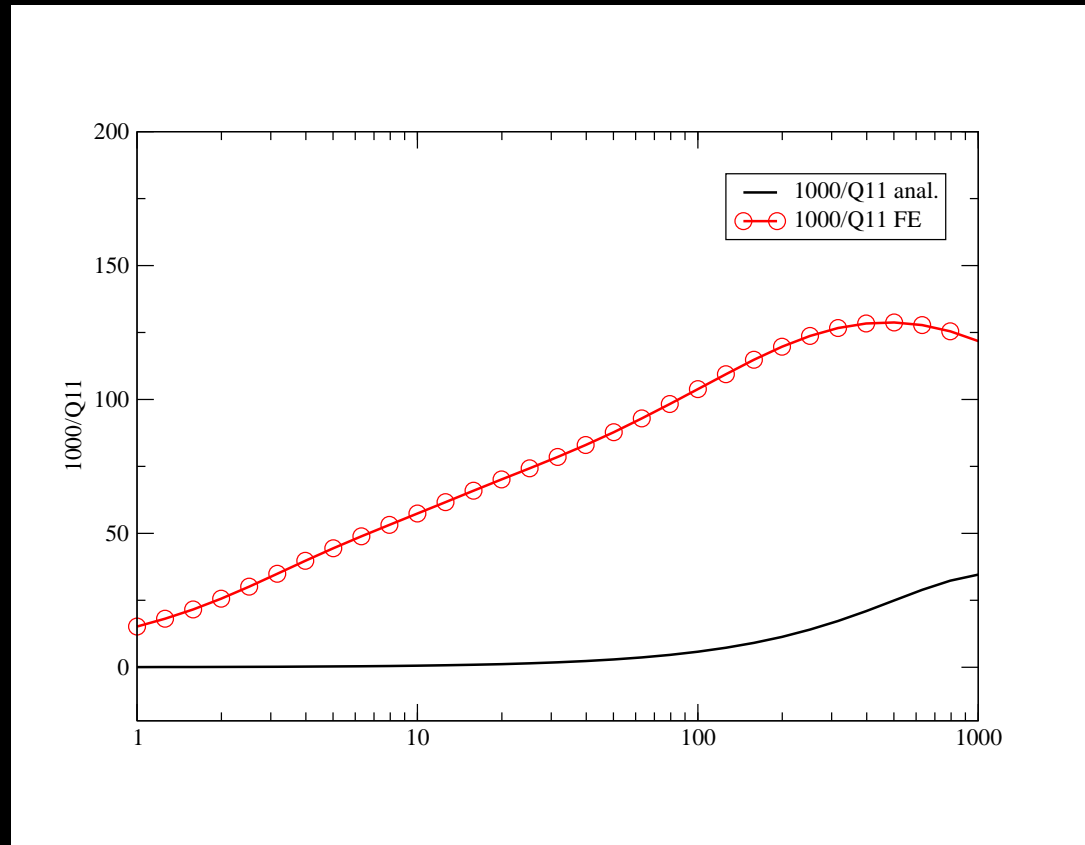


PATCHY SATURATION. P-wave phase velocities parallel (V_{p11}) to the layering plane.



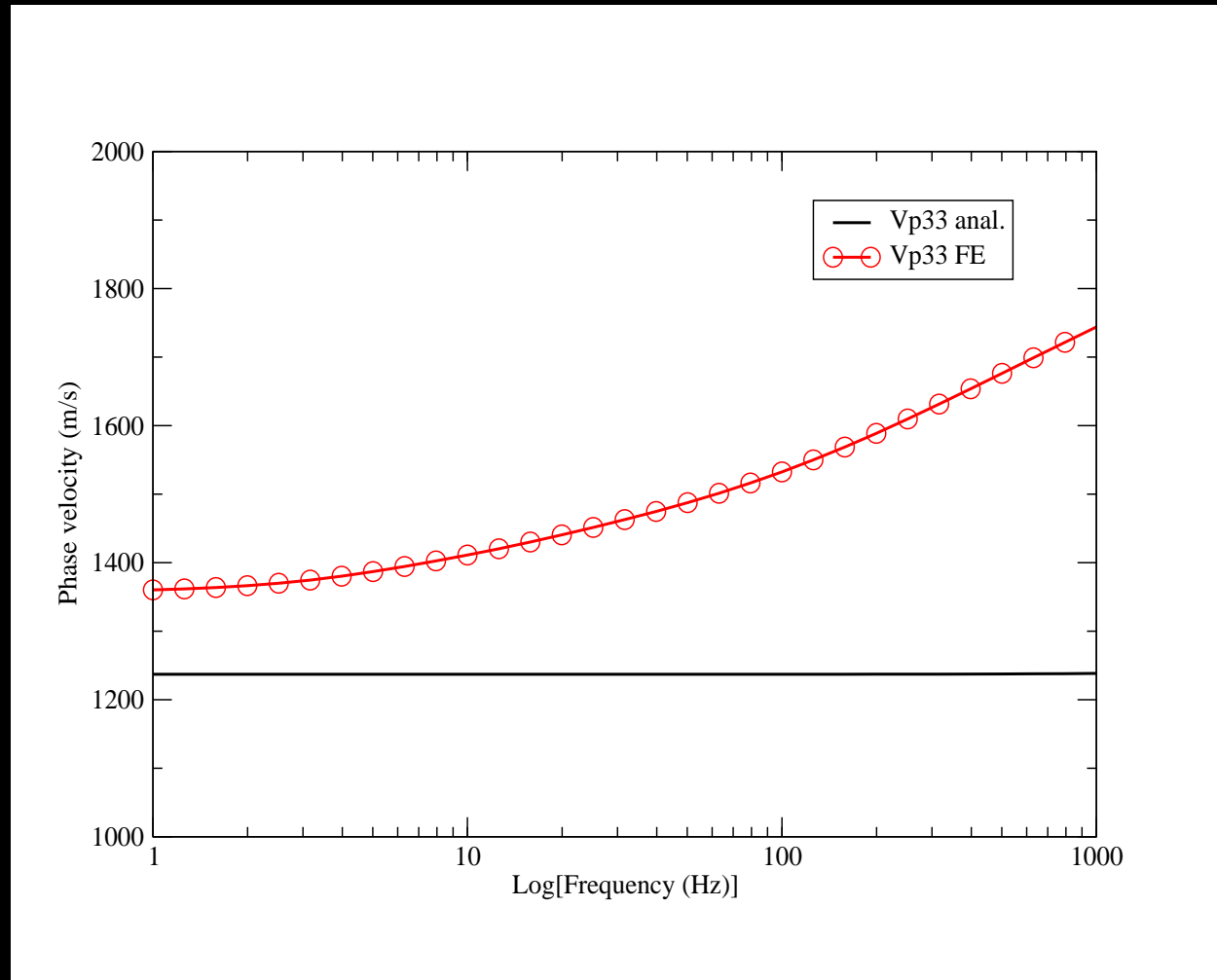
Sequence of 5 cm patchy-saturated Utsira and 1 cm brine-saturated mud . The Analytical curve corresponds to the same sequence but for CO₂-saturated Utsira.

PATCHY SATURATION. Dissipation factors parallel ($1000/Q_{11}$) to the layering plane.



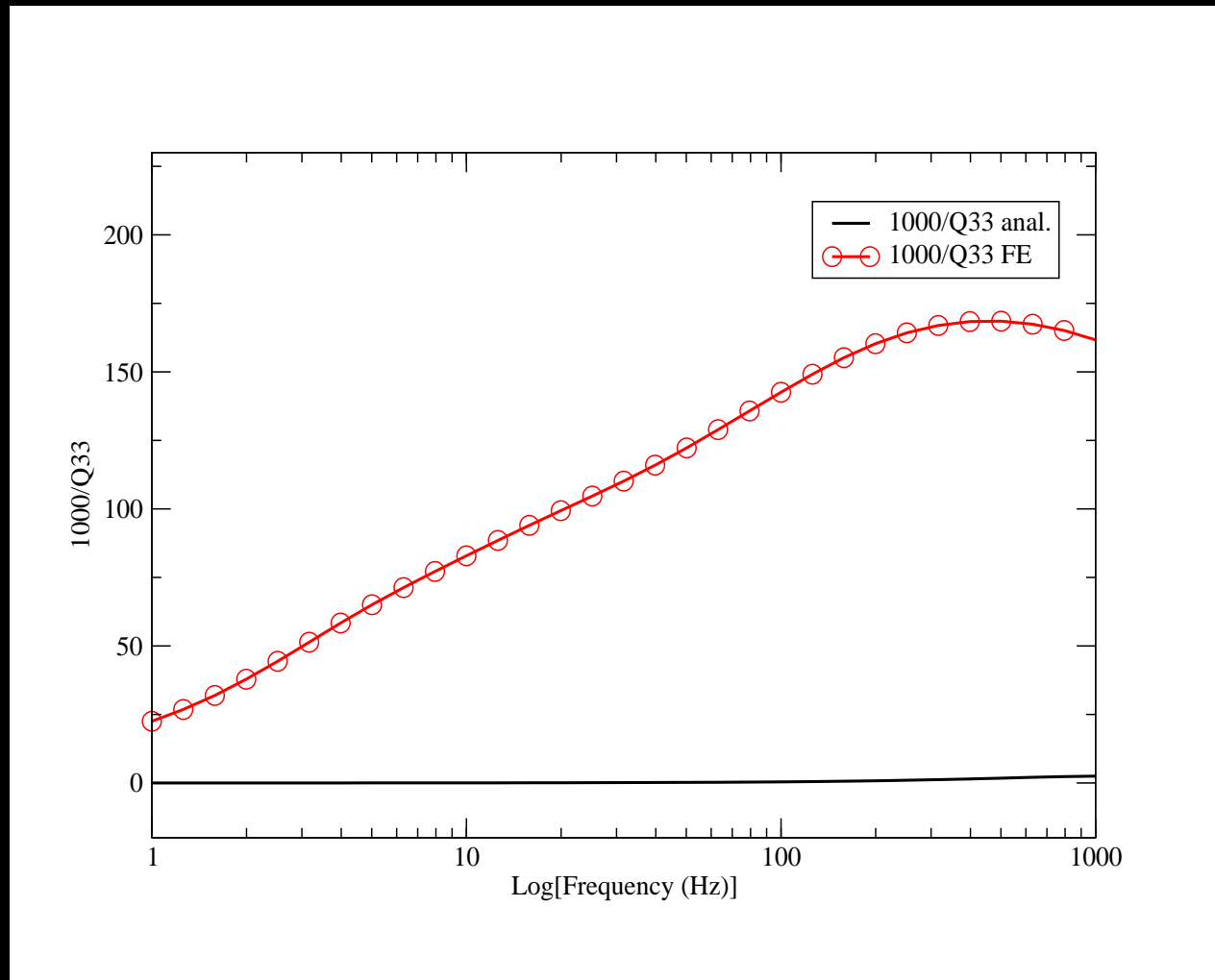
Sequence of 5 cm patchy-saturated Utsira and 1 cm brine-saturated mud . The Analytical curve corresponds to the same sequence but for CO_2 -saturated Utsira.

PATCHY SATURATION. P-wave phase velocities perpendicular (V_{p33}) to the layering plane.



Sequence of 5 cm patchy-saturated Utsira and 1 cm brine-saturated mud . The Analytical curve corresponds to the same sequence but for CO_2 -saturated Utsira.

PATCHY SATURATION. Dissipation factors perpendicular (1000/Q33) to the layering plane.



Sequence of 5 cm patchy-saturated Utsira and 1 cm brine-saturated mud . The Analytical curve corresponds to the same sequence but for CO₂-saturated Utsira.

CONCLUSIONS. I

- We presented a novel numerical FEM to obtain the complex and frequency-dependent stiffnesses of a VTI homogeneous medium equivalent to a finely layered Biot's medium.
- The methodology is based on the FE solution Biot's equation in the space-frequency domain to simulate harmonic compressibility and shear tests.
- The FE results were checked against a theory valid for laterally homogeneous layers and 1D-fluid-flow direction.

CONCLUSIONS. II

- Velocity and attenuation anisotropy can be observed in the qP and qSV wave modes, with attenuation higher along the layering plane for the case being analyzed.
- SV-Shear attenuation is much weaker than the qP attenuation, and SH waves are lossless.
- The FEM was applied to determine a VTI homogeneous medium equivalent to a finely layered patchy-saturated Biot's medium.
- THANKS FOR YOUR ATTENTION.